

**Two-electron states of a group-V donor in silicon from atomistic full configuration interactions**Archana Tankasala,<sup>1,\*</sup> Joseph Salfi,<sup>2</sup> Juanita Bocquel,<sup>2</sup> Benoit Voisin,<sup>2</sup> Muhammad Usman,<sup>3</sup> Gerhard Klimeck,<sup>1</sup> Michelle Y. Simmons,<sup>2</sup> Lloyd C. L. Hollenberg,<sup>3</sup> Sven Rogge,<sup>2</sup> and Rajib Rahman<sup>1,†</sup><sup>1</sup>*Network for Computational Nanotechnology, Purdue University, West Lafayette, Indiana 47907, USA*<sup>2</sup>*Centre for Quantum Computation and Communication Technology, School of Physics, The University of New South Wales, Sydney, 2052 New South Wales, Australia*<sup>3</sup>*Centre for Quantum Computation and Communication Technology, School of Physics, The University of Melbourne, Parkville, 3010 Victoria, Australia*

(Received 14 March 2017; revised manuscript received 22 March 2018; published 2 May 2018)

Two-electron states bound to donors in silicon are important for both two-qubit gates and spin readout. We present a full configuration interaction technique in the atomistic tight-binding basis to capture multielectron exchange and correlation effects taking into account the full band structure of silicon and the atomic-scale granularity of a nanoscale device. Excited  $s$ -like states of  $A_1$  symmetry are found to strongly influence the charging energy of a negative donor center. We apply the technique on subsurface dopants subjected to gate electric fields and show that bound triplet states appear in the spectrum as a result of decreased charging energy. The exchange energy, obtained for the two-electron states in various confinement regimes, may enable engineering electrical control of spins in donor-dot hybrid qubits.

DOI: [10.1103/PhysRevB.97.195301](https://doi.org/10.1103/PhysRevB.97.195301)**I. INTRODUCTION**

Quantum computing device architectures based on donors in silicon have attracted considerable attention in recent times [1]. Electrons bound to phosphorous donors in silicon have long decoherence times [2,3] due to weak spin-orbit coupling and the small fraction of spin-carrying isotopes of silicon. In addition to the well-studied neutral donor state  $D^0$  of a group-V donor in silicon, the two-electron negatively charged donor state  $D^-$  is of technological relevance [4–13].

The two-electron states of donors are important for spin readout through spin-to-charge conversion [4–6] and spin-dependent tunneling [10] and also for tuning the exchange coupling in two qubits towards the charge-transfer regime [12]. Recent experiments have also used the two-electron donor state with a bound hole for addressing nuclear spins [14,15]. Moreover, the two-electron donor states are also observed in quantum transport in extremely scaled field-effect transistors [7–9] and in artificially patterned dopant arrays that provide access to impurity Hubbard bands [13,16]. Two-electron energy spectra and wave functions in all of the above-mentioned references are determined primarily by the electron-electron interactions, including the Coulomb repulsion, exchange, and correlations. Knowledge of how to engineer these interactions may help in the experimental realization of such proposals in various quantum devices.

Recent schemes to form hybrid donor-dot qubit systems [11] that pulse electrons between donors and interface confined states also benefit from an understanding of  $D^-$  in a gated nanoscale environment. The  $Z$ -gate operation in such qubits is realized by electrically tuning the exchange interaction

between the singlet and triplet basis states. Precise knowledge of the two-electron states, exchange couplings, and various orbital and spin components of the two-electron wave functions is therefore critical for understanding and engineering gate operations and for optimizing qubit metrics such as relaxation and coherence times.

Two-electron states of donors in silicon, both in bulk and close to the oxide-semiconductor interfaces, have previously been studied from a self-consistent Hartree approach using tight-binding wave functions [17] and also variationally with Chandrasekhar-type wave functions [18] to obtain ground states and charging energies. However, these approximate methods consider only Coulomb repulsion between electrons or treat higher-order exchange-correlations only approximately. Consequently, the excited states of a two-electron system and the singlet-triplet splitting of relevance to qubits cannot be evaluated accurately from these models. In this work, we compute the two-electron states of the donor in a device-like environment from an atomistic full configuration interaction (FCI) method, which also provides excited states and exchange energies as a function of gate fields and donor locations. Moreover, we are able to evaluate the contribution of the various donor orbital and valley states to the two-electron state and show how the charging and exchange energies change with applied electric fields and donor depths in a device. With increasing electric field, we see the exchange changes nonmonotonically for the donor-hybrid-interface sequence with applied fields. The results show how exchange energy between electrons confined in donors and interface states can be tuned in a hybrid donor-dot setting.

The electronic structure of a group-V donor in silicon is complicated by the sixfold conduction-band valley degeneracy of silicon. The tetrahedral symmetry of the crystal and central-cell corrections [19] lift the valley degeneracies and cause

\*atankas@purdue.edu

†rrahman@purdue.edu

donor states to form hybrid valley-orbit states with species-dependent level splittings [20]. We employ a multimillion-atom tight-binding model to capture the peculiar electronic structure of the donor, which is also affected by fields and interfaces present in a nanoscale device [21]. We use these donor states as basis functions to solve the two-electron problem from FCI, which provides converged two-electron states and their configurations in terms of Slater determinants [22]. In this way, we include atomistic details of the silicon crystal and the nanodevice in a description of exchange and correlation energies. This enables us to analyze the two-electron donor states in great detail and to gain insight on how to engineer them for single-atom electronics in silicon.

## II. METHODOLOGY

Single-electron states of a single donor are obtained from the atomistic tight-binding (TB) approach [23]. The method is shown to correctly determine the  $D^0$  binding energies of the donor and its excited states [24], using a central-cell model with optimized parameters for on-site cutoff potential  $U_0$  and on-site orbital energies  $E_s$  and  $E_p$  [25]. These are used as a basis to construct the many-electron antisymmetric Slater determinants. In FCI, a multielectron state is a superposition of different Slater configurations. Excited configurations arising from exciting electrons to virtual orbitals are considered to include higher-order correlations. The multiply excited Slater determinants form a complete basis set in the function space spanned by the single-electron states. The FCI wave function for an  $n$ -electron system formed from a basis of  $N$  single-electron states is expressed as

$$|\Psi(\vec{r}_1, \dots, \vec{r}_n)\rangle = C_0|\Psi_0\rangle + \sum_{a,r} C_a^r |\Psi_a^r\rangle + \sum_{ab,rs} C_{ab}^{rs} |\Psi_{ab}^{rs}\rangle + \dots,$$

where  $|\Psi_0\rangle$  is the ground-state Slater determinant from  $n$  occupied orbitals  $|ab\dots c\rangle$ ,  $|\Psi_a^r\rangle$  are singly excited Slater determinants from promoting the electron in state  $\psi_a$  to the excited state  $\psi_r$ ,  $|rb\dots c\rangle$ ,  $|\Psi_{ab}^{rs}\rangle$  are doubly excited Slater determinants from promoting electrons in states  $\psi_a$  and  $\psi_b$  to excited states  $\psi_r$  and  $\psi_s$ , and so on [22].  $C_i$  are the corresponding coefficients of these Slater determinants. The multielectron state, expanded in this basis, gives a more complete quantitative description of the configurations that contribute to the many-electron states.

In the basis of possible  $n$ -electron Slater determinants  $|A\rangle = |\psi_i\psi_j\dots\rangle$  and  $|B\rangle = |\psi_k\psi_l\dots\rangle$ , the Hamiltonian element  $\mathcal{H}(a,b)$  is  $\langle\psi_i\psi_j\dots|\mathcal{H}|\psi_k\psi_l\dots\rangle$ , where  $\psi_x$  are the single-electron states of the system in the basis of localized atomic orbitals of each atom in the crystal, as obtained from the atomistic TB method [26]. Electron-electron interactions in the Hamiltonian are of the form

$$\langle\psi_i\psi_j|\frac{e^2}{4\pi\epsilon|\vec{r}_1-\vec{r}_2}| \psi_k\psi_l\rangle,$$

which needs an evaluation of Coulomb and exchange integrals,

$$J = \iint_V \psi_i^*(\vec{r}_1)\psi_j^*(\vec{r}_2)\frac{e^2}{4\pi\epsilon|\vec{r}_1-\vec{r}_2} \psi_k(\vec{r}_1)\psi_l(\vec{r}_2) d\vec{r}_1 d\vec{r}_2,$$

$$K = \iint_V \psi_i^*(\vec{r}_1)\psi_j^*(\vec{r}_2)\frac{e^2}{4\pi\epsilon|\vec{r}_1-\vec{r}_2} \psi_l(\vec{r}_1)\psi_k(\vec{r}_2) d\vec{r}_1 d\vec{r}_2,$$

respectively, for each Hamiltonian element. Here,  $\vec{r}_1$  and  $\vec{r}_2$  are the coordinates of the two electrons,  $V$  is the simulation domain,  $e$  is the electronic charge, and  $\epsilon$  is the dielectric constant of the host material.

Both  $J$  and  $K$  are double integrals over the entire region of the simulation domain. The evaluation of these integrals and the construction of an atomistic FCI Hamiltonian is computationally more expensive than the diagonalization of the FCI Hamiltonian to obtain multielectron energies and wave functions. The computation is massively parallelized for large systems with many single-electron states in the basis. The integrals, defining an  $n$ -body problem, are evaluated using the fast multipole method (FMM) [27] to reduce the computational complexity when a high accuracy in the energies is not required. For a high accuracy in the solution, on the scale of  $\mu\text{eV}$ , FMM and brute-force calculations have the same computational burden. Solving the FCI Hamiltonian gives the energies of the multielectron states and the contributions from the possible Slater configurations to each of these states.

The binding energy  $D_{\text{BE}}^-$  and charging energy  $D_{\text{CE}}^-$  of the two-electron state are calculated from the two-electron ground state  $D_{\text{GS-FCI}}^-$  obtained from atomistic FCI, the conduction-band minima of silicon ( $\text{CB}_{\text{min}}$ ), and the single-electron ground state  $D_{\text{GS-TB}}^0$  obtained from tight-binding simulations using the equations

$$D_{\text{BE}}^- = D_{\text{GS-FCI}}^- - \text{CB}_{\text{min}} - D_{\text{GS-TB}}^0,$$

$$D_{\text{CE}}^- = D_{\text{GS-FCI}}^- - 2D_{\text{GS-TB}}^0.$$

For donors located close to a Si-SiO<sub>2</sub> interface in a metal-oxide-semiconductor (MOS) device, the electrostatics of the metal-insulator-silicon considerably influences the energy spectrum of the donor, especially for a negative donor. The dielectric mismatches renormalize the electron-electron interaction. This effect can be captured in the atomistic FCI using the method of images charges. Here, the Coulomb and exchange interactions of the electron are evaluated not only between two electrons but also between an electron and the images of the other electron. Benchmarking the potential profile of a point charge from the analytical method of image charges with COMSOL simulation software suggests that at least ten images of each electron must be considered in the analytical method to obtain the correct potential. This considerably increases the computational burden in evaluating each matrix element of the FCI Hamiltonian. However, the inclusion of these image charges to capture the screening of electron interactions is necessary for an accurate quantitative evaluation of the two-electron states of the subsurface donor. A similar method, tight binding with FCI, used fast Fourier transforms to solve for the two-electron integrals and applied the method to study two-electron quantum dot states [28].

Interface donor systems have previously been studied for arsenic donors in silicon using the self-consistent Hartree approach [17]. This method is shown to give a good estimate of the  $D^-$  binding energies in 10–20 iterations, but exchange correlations are ignored, and the excited two-electron states and their configurations may not be exactly determined from this method. The Hartree method self-consistently updates the basis in several iterations. However, in general, FCI does not scale well with the number of electrons.

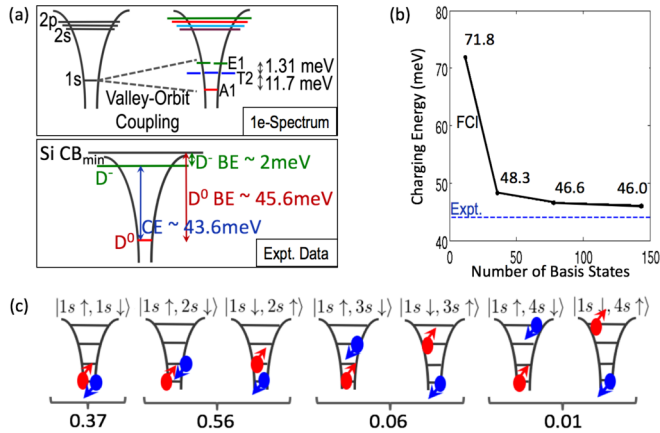


FIG. 1. Two-electron state of a bulk P donor in silicon. (a) Degeneracy of hydrogenic  $1s$ -like states of a donor Coulomb confinement potential, broken into valley-orbit singlets, triplets, and doublets ( $A_1$ ,  $T_2$ , and  $E$ , respectively) by the tetrahedral crystal symmetry of the host material. Binding and charging energies of donor bound electrons are from experimentally observed  $D^0$  and  $D^-$  states. (b)  $D^-$  charging energy of the phosphorous donor in silicon converges towards the experimentally observed value of 43.6 meV [31] with an increasing number of single-electron states in the FCI basis. The data points correspond to the inclusion of  $1s$ -,  $2s$ -,  $3s$ -, and  $4s$ -like states in the basis. (c) Two-electron  $D^-$  ground state. Numbers indicate the probability that the system is in each of the configurations. One of the electrons is always in the  $D^0$  ground state, the  $1s$ -like state with  $A_1$  symmetry. The second electron occupies  $2s$ -,  $3s$ -, or  $4s$ -like excited states also of  $A_1$  symmetry. The excited-state splittings corresponding to  $2s$ ,  $3s$ , and  $4s$  are magnified in the schematic relative to (a) to portray the electronic configurations clearly. Also, the  $T_2$  and  $E_1$  states are omitted for simplicity.

### III. RESULTS AND ANALYSIS

The electronic spectrum of a single donor in a tetrahedrally symmetric crystal potential of silicon is modified by valley-orbit coupling. Here the sixfold valley degeneracy of the ground state, the  $1s$  manifold, of donor Coulomb confinement is broken by the local crystal field into a singlet with  $A_1$  symmetry, a triplet with  $T_2$  symmetry, and a doublet with  $E$  symmetry, as shown in Fig. 1(a). The binding energies and degeneracies of these  $1s$  states of a phosphorous donor in silicon, the  $D^0$  center, have been determined using the semiempirical tight-binding model and have successfully been validated against experimental values [24,29]. For donors in the vicinity of a gate, the Stark shifted donor spectrum calculated using the tight-binding method also agrees closely with the experiments [30].

In this work,  $D^-$  centers are studied using atomistic FCI, and the two-electron charging energies of bulk and interface donors are compared against available experimental values. Excited states of the donor spectrum ( $2p$ ,  $2s$ , ..., up to  $4s$ ) and their degeneracies are also resolved from the eigensolver and are crucial to solve the two-electron problem, as will be shown later.

#### A. Negative donor in bulk

Optical experiments on a bulk phosphorous donor in silicon indicate the presence of a bound singlet  $D^-$  state with a binding

energy approximately 2.0 meV below the conduction-band minimum, corresponding to a charging energy of 43.6 meV [31]. Figure 1 presents the atomistic FCI calculation of a bulk phosphorous donor  $D^-$  in silicon. It must be noted that although we treat the phosphorous donor specifically here, the same method can be used for other shallow group-V donors in silicon, and the results will qualitatively be the same. Figure 1(b) shows the charging energy of the two-electron state as a function of the number of spin-resolved  $D^0$  atomic states in the basis. Including only  $1s$ -like  $D^0$  states in the atomistic FCI method gives a significantly overestimated charging energy of 71.8 meV, as shown in Fig. 1(b), indicating an incomplete basis. With the inclusion of  $2s$ -,  $3s$ -, and  $4s$ -like  $D^0$  states in the basis, the charging energy converges to 46.0 meV. It must be noted that the binding energies are evaluated with reference to the conduction-band minima of bulk silicon at 1.131355 eV obtained from a bulk band structure calculation [32]. A finite box size of the simulation domain, in this case  $35 \times 35 \times 35 \text{ nm}^3$ , causes interface confinement effects on the excited donor states. Therefore, the system is not really bulk, only bulklike, which leads to higher orbital energies due to increased confinement. This is one of the reasons for the slightly higher charging energy of 46.0 meV relative to the 43.6 meV measured in the optical experiments. From the wave function, the  $D^-$  state with 46.0 meV charging energy is observed to be localized to the donor. Within the approximations of tight-binding basis orbitals, discretized tight-binding wave functions, central-cell corrected donor potential, and truncated single-electron basis set, atomistic FCI still gives a fairly close charging energy of the negative phosphorous donor in bulk. Hence, the excited donor states in the manifold of  $2p$ ,  $2s$ ,  $3s$ , and so on, which are typically ignored in most calculations, are crucial for the solution of the two-electron donor state.

Figure 1(c) shows the two-electron configurations that compose the singlet  $D^-$  ground state of a phosphorous donor in silicon as obtained from FCI. From the two-electron FCI wave function, it is seen that the probability of the  $D^-$  state existing in the  $|1s \uparrow, 1s \downarrow\rangle$  configuration is only 37%. The  $1s$ -like states are therefore not sufficient to describe the  $D^-$  ground state. There is a significant contribution of 56% from  $|1s \uparrow, 2s \downarrow\rangle$  and  $|1s \downarrow, 2s \uparrow\rangle$  states, and including the  $2s$ -like states in the FCI basis corrects the charging energy. Contributions from  $2s$ -,  $3s$ -, and  $4s$ -like  $D^0$  states to the  $D^-$  ground state suggests that the negative donor has strong Coulomb correlations. A complete basis for such a system is huge and requires at least 150 single-electron spin states. For the employed basis and simulation domain, the calculated atomistic FCI charging energy (46.0 meV) approaches the value in bulk (43.6 meV). The remaining discrepancy is small and might be reduced by increasing the basis size or simulation domain size. However, increasing either is beyond the scope of the present work.

As can be seen from Fig. 1(c), all the contributing electronic configurations have antiparallel spins, consistent with the net spin of a singlet state. Moreover, we find that one of the electrons of  $D^-$  always occupies the  $1s$ -like state with  $A_1$  symmetry, the  $D^0$  ground state. It is favorable for the other electron to have the same valley symmetry, which increases the electron correlations, thus lowering the energy of the two-electron singlet state. From the FCI solution of the ground

state, we find that  $2s$ -,  $3s$ -, and  $4s$ -like  $D^0$  states that contribute to the  $D^-$  singlet all have  $A_1$  symmetry. Therefore, for the bulk donor,  $T_2$  and  $E$  states with different valley symmetries are not found to contribute to the  $D^-$  ground state. It must be noted that the  $D^-$  state from atomistic FCI is somewhat like the Chandrasekhar-like wave function with appropriate valley symmetries if the second orbital of the Chandrasekhar wave function can be thought of as a hybrid of the  $1s$ ,  $2s$ ,  $3s$ , and  $4s$  orbitals.

The significant contributions of the excited Slater determinants to the  $D^-$  state show strong electronic correlations based on orbital and valley symmetries. Such correlations cannot be captured by treating the problem using Hartree self-consistently. Atomistic FCI, therefore, provides a comprehensive description and valuable insights into the two-electron states of donors in silicon taking into account the electron-electron interactions arising from excited configurations that cannot be ignored for a correlated system.

### B. Negative donor close to the interface

Donors close to the oxide-silicon interface are important for silicon quantum computing for a number of reasons. The first signature of single-donor orbital states and their Stark shift were detected in single donors located less than 10 nm from an oxide-silicon interface in Fin Field-Effect Transistors (FinFETs) [9]. In this regime, the donor is strongly tunnel coupled to states confined at the interface, and a gate voltage can ionize the electron adiabatically through intermediate donor-interface/donor-dot hybrid states [17,33]. There have been proposals to use this system to form hybrid donor-dot qubits where electrons are pulsed to the interface states for two-qubit operations with enhanced exchange couplings and pulsed back to the donors to take advantage of the long quantum memory in donor bound states [34,35]. Recent experiments have also manipulated multiple electrons between donors and interface states [11] in a hybrid donor-dot setting.

Two-electron charging energies of subsurface dopants have also been observed to be around 30 meV [9], in stark contrast to bulk charging energies close to 44 meV. This also enables the possibility of bound triplet states, which to our knowledge have not been observed in bulk donors, and a measurable singlet-triplet (exchange) splitting. Here, we show FCI can explain these experimental observations. We will also show the change in exchange coupling in a two-electron donor state as a function of an applied bias for donors close to interfaces, which is of relevance in hybrid donor-dot qubits.

The binding energies of both  $D^0$  and  $D^-$  states are plotted in Fig. 2(a). The difference between the two is the charging energy of  $D^-$ , shown by a dashed line on the right axis. Singlet-triplet splitting or the exchange energy, with varying electric field, is shown in Fig. 2(b). Exchange depends on the overlap of the single-electron wave functions. Charge densities of the  $D^-$  ground state are shown in Fig. 2(c), revealing the spatial spread of two-electron states under different confinement regimes.

Increasing the electric field causes the excited donor states to hybridize with the interface well states. One of the electrons is pushed towards the interface, leading to delocalization of the electron, as shown in the schematic for the hybrid regime in Fig. 2(a). With increasing field in this regime (at moderate

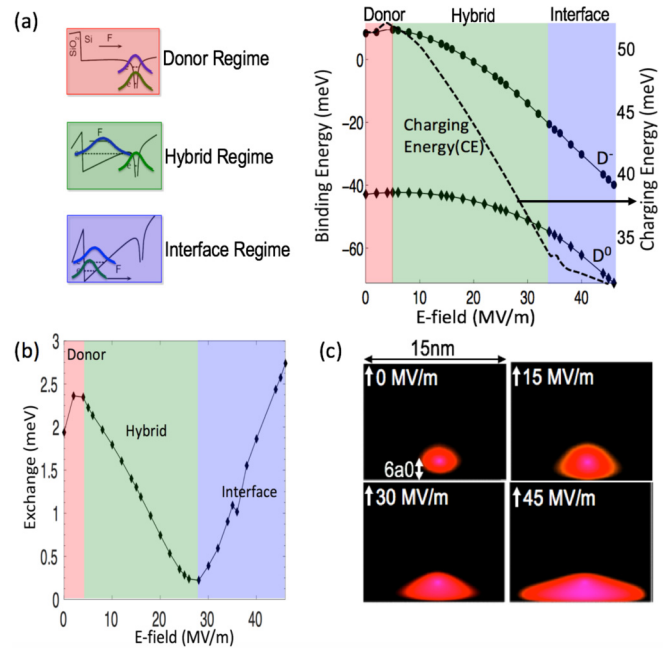


FIG. 2. Effect of electric field on the charging and exchange energies of a P donor in silicon,  $6a_0$  deep from the oxide-semiconductor interface. (a) Schematic of possible regimes with increasing  $E$  fields when both electrons are localized at the donor, one electron is at the donor and the other is hybridized with the interface, both electrons are at the interface.  $D^0$  and  $D^-$  binding energies and derived  $D^-$  charging energy (dashed line) with increasing electric fields are shown. (b) Exchange or singlet-triplet splitting of the  $D^-$  state. (c) Two-electron densities of the  $D^-$  singlet ground state from the full configuration interaction for different confinement regimes (on a log scale). Delocalization of two-electron states is observed at large fields.

electric fields) the delocalization increases, which lowers the charging energy. This delocalization also lowers the overlap of the electron wave functions, thus decreasing the exchange with increasing fields.

At large fields, both electrons dominantly occupy the ground state of the interface well, strongly confined along the vertical field direction and weakly confined by the donor potential laterally. The decrease in orbital energies of single-electron states with increasing field leads to the decrease in the charging energy of  $D^-$  in the interfacial regime. However, the increase in wave-function overlap of the two electrons localized at the interface causes an increase in exchange with increasing electric field. The donor regime at low electric fields is similar to the interface regime, where both electrons are localized at the donor instead of the interface. A donor-dot hybrid singlet-triplet qubit can be operated on either side of the minimum point in the  $J$  vs  $E$  curve, depending on whether initialization and readout are done in the donor (2,0) or interface (0,2) states. If high electric fields are to be avoided, then the optimum point to operate the qubit is to have two electrons localized in the two potential wells and reduce the vertical  $E$  fields to push the interface electron to the (2,0) states of the donor.

$D^-$  charging and exchange energies varying with depth of the P donor are shown in Fig. 3, corresponding to the hybrid regime. At 15 MV/m field, as can be understood from the schematic in Fig. 3(a), increasing the depth of the

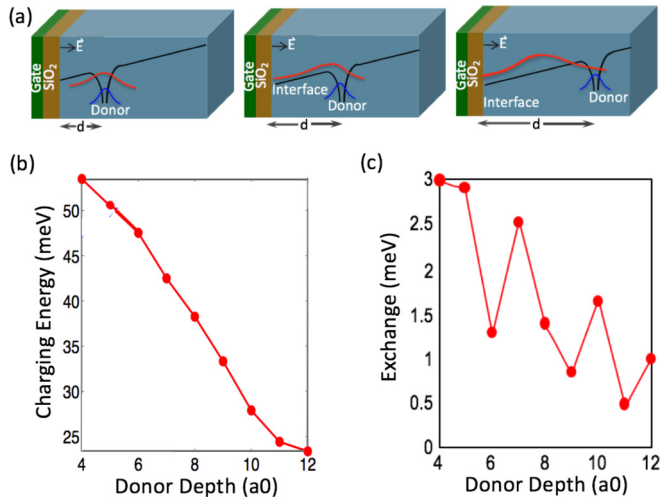


FIG. 3. Effect of the donor depth on the charging and exchange energies. (a) Schematic of increasing electron delocalization with increasing donor depth at a moderate electric field of 15 MV/m in the hybrid regime. (b)  $D^-$  charging energies. (c) Singlet-triplet splitting of  $D^-$  ( $a_0 = 0.543$  nm for silicon).

donor increases the delocalization of one of the electrons, thus lowering the charging energies, as seen in Fig. 3(b). This also leads to a smaller overlap of electron wave functions, and therefore, exchange also decreases with increasing donor depth, as shown in Fig. 3(c). The oscillations in exchange are due to the difference in phase of the Bloch wave functions of the two electrons and are within the same order of magnitude. Comparatively, the electric field tunability of the exchange as shown in Fig. 2(b) is one order of magnitude at a depth of 3.26 nm (or  $6a_0$ ). This shows that for a donor-dot hybrid qubit [11], the  $Z$ -gate operation, which depends on the singlet-triplet splitting, will be less sensitive (less than an order of magnitude) to the precise placement of the donor perpendicular to the interface and therefore can be strongly tuned by the gate field. Moreover, given that the interface regime appears at larger electric fields for shallower donors, the slope of the  $J$  vs detuning, or  $\partial J/\partial E$ , in the hybrid regime is smaller for shallow donors, thus potentially leading to a reduced charge noise.

Donors close to the interface have dielectric mismatches arising from Si-SiO<sub>2</sub> and SiO<sub>2</sub>-metal gate interfaces. A reservoir of heavily doped silicon substrate also creates a dielectric mismatch, as shown in Fig. 4(a). The reservoir is particularly important in scanning tunneling experiments when the highly doped silicon layer is located 10–20 nm away from the donor [36,37]. For MOS-like devices, the device contacts are in proximity to the donor too, and ideally, the image charges in contacts, which have been ignored in this work, must be accounted for as well [38]. Metallic and oxide interfaces close to an electron affect the electrostatics of the system and screen the electron-electron repulsions, thus lowering the two-electron energies of the system. Figure 4(b) shows the effect of the electrostatics of interfaces on the charging energy of the  $D^-$  state. As the thickness of the SiO<sub>2</sub> oxide layer decreases, the Si-SiO<sub>2</sub>-metal interface becomes more metallic in nature and screens the electron interactions, resulting in decreasing the two-electron charging energy. The effect of

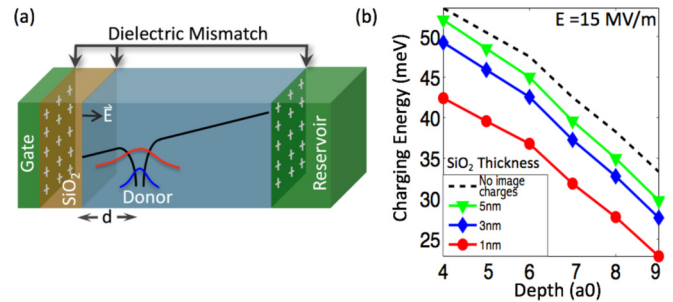


FIG. 4. Heterointerface effects on donor charging energy. (a)  $P$  donor in silicon, located close to the Si-SiO<sub>2</sub>-metal interface and to a heavily doped reservoir, which is important in resonant tunneling experiments. (b) Charging energy of  $D^-$  at 15 MV/m  $E$  field for different oxide thicknesses. A thinner dielectric increases the screening of electronic repulsions by the metallic gate, leading to lower charging energies.

the image charges is seen mainly as an offset in the charging energy.

#### IV. CONCLUSION

Atomistic FCI simulations demonstrate that the bulk  $D^-$  is a highly correlated state with significant contributions from higher  $s$ -like  $D^0$  orbitals of  $A_1$  symmetry to the two-electron singlet state. The charging energy of a bulk negative donor is significantly overestimated without the inclusion of these excited levels. For shallow donors, the charging and exchange energies are shown to be sensitive to the depth of the donors from the Si-SiO<sub>2</sub> interface, applied electric fields, and the electrostatics of the interfaces from the atomistic FCI simulations. The charging and exchange energies of  $D^-$  are lower for deeper donors under moderate electric fields, typically the regime of interest for hybrid donor-dot architectures, but the exchange energies show small oscillations, less than an order of magnitude, with increasing depth. Moreover, in spite of the increased computational complexity in including the effect of electrostatics of interfaces on electron interactions, they are significant in evaluating the charging energies of shallow donors in the vicinity of oxide and metallic interfaces. The understanding of two-electron states from this work may be useful in the realization of hybrid donor-dot qubit architectures.

#### ACKNOWLEDGMENTS

This work is funded by the ARC Center of Excellence for Quantum Computation and Communication Technology CE1100001027 and in part by the U.S. Army Research Office (Grant No. W911NF-13-1-0024). M.Y.S. acknowledges an ARC Laureate Fellowship. Computational resources from NCN/Nanohub are acknowledged. This work is also part of the Accelerating Nano-scale Transistor Innovation with NEMO5 on Blue Waters PRAC allocation support by the National Science Foundation (Grant No. OCI-0832623). This work used over 60000 CPU hours on SDSC Comet at the Extreme Science and Engineering Discovery Environment (XSEDE), which is supported by National Science Foundation Grant No. ECS150001 [39].

- [1] B. E. Kane, A silicon-based nuclear spin quantum computer, *Nature (London)* **393**, 133 (1998).
- [2] A. M. Tyryshkin, S. Tojo, J. J. Morton, H. Riemann, N. V. Abrosimov, P. Becker, H.-J. Pohl, T. Schenkel, M. L. Thewalt, K. M. Itoh *et al.*, Electron spin coherence exceeding seconds in high-purity silicon, *Nat. Mater.* **11**, 143 (2012).
- [3] M. Veldhorst, J. Hwang, C. Yang, A. Leenstra, B. De Ronde, J. Dehollain, J. Muhonen, F. Hudson, K. M. Itoh, A. Morello *et al.*, An addressable quantum dot qubit with fault-tolerant control-fidelity, *Nat. Nanotechnol.* **9**, 981 (2014).
- [4] B. Kane, Electron Devices for Single Electron and Nuclear Spin Measurement, US Patent No. 6,369,404 (2002).
- [5] L. C. L. Hollenberg, C. J. Wellard, C. I. Pakes, and A. G. Fowler, Single-spin readout for buried dopant semiconductor qubits, *Phys. Rev. B* **69**, 233301 (2004).
- [6] A. D. Greentree, A. R. Hamilton, L. C. L. Hollenberg, and R. G. Clark, Electrical readout of a spin qubit without double occupancy, *Phys. Rev. B* **71**, 113310 (2005).
- [7] H. Sellier, G. P. Lansbergen, J. Caro, S. Rogge, N. Collaert, I. Ferain, M. Jurczak, and S. Biesemans, Transport Spectroscopy of a Single Dopant in a Gated Silicon Nanowire, *Phys. Rev. Lett.* **97**, 206805 (2006).
- [8] M. Pierre, R. Wacquez, X. Jehl, M. Sanquer, M. Vinet, and O. Cueto, Single-donor ionization energies in a nanoscale CMOS channel, *Nat. Nanotechnol.* **5**, 133 (2010).
- [9] G. P. Lansbergen, R. Rahman, J. Verduijn, G. C. Tettamanzi, N. Collaert, S. Biesemans, G. Klimeck, L. C. L. Hollenberg, and S. Rogge, Lifetime-Enhanced Transport in Silicon Due to Spin and Valley Blockade, *Phys. Rev. Lett.* **107**, 136602 (2011).
- [10] T. F. Watson, B. Weber, M. G. House, H. Büch, and M. Y. Simmons, High-Fidelity Rapid Initialization and Read-Out of an Electron Spin via the Single Donor  $D^-$  Charge State, *Phys. Rev. Lett.* **115**, 166806 (2015).
- [11] P. Harvey-Collard, N. T. Jacobson, M. Rudolph, J. Dominguez, G. A. T. Eyck, J. R. Wendt, T. Pluym, J. K. Gamble, M. P. Lilly, M. Pioro-Ladrière *et al.*, Nuclear-driven electron spin rotations in a single donor coupled to a silicon quantum dot, *Nat. Commun.* **8**, 1029 (2017).
- [12] Y. Wang, A. Tankasala, L. C. Hollenberg, G. Klimeck, M. Y. Simmons, and R. Rahman, Highly tunable exchange in donor qubits in silicon, *npj Quantum Inf.* **2**, 16008 (2016).
- [13] E. Prati, K. Kumagai, M. Hori, and T. Shinada, Band transport across a chain of dopant sites in silicon over micron distances and high temperatures, *Sci. Rep.* **6**, 19704 (2016).
- [14] M. Steger, K. Saeedi, M. Thewalt, J. Morton, H. Riemann, N. Abrosimov, P. Becker, and H.-J. Pohl, Quantum information storage for over 180 s using donor spins in a  $^{28}\text{Si}$  semiconductor vacuum, *Science* **336**, 1280 (2012).
- [15] K. Saeedi, S. Simmons, J. Z. Salvail, P. Dluhy, H. Riemann, N. V. Abrosimov, P. Becker, H.-J. Pohl, J. J. Morton, and M. L. Thewalt, Room-temperature quantum bit storage exceeding 39 minutes using ionized donors in silicon-28, *Science* **342**, 830 (2013).
- [16] J. Salfi, J. Mol, R. Rahman, G. Klimeck, M. Simmons, L. Hollenberg, and S. Rogge, Quantum simulation of the hubbard model with dopant atoms in silicon, *Nat. Commun.* **7**, 11342 (2016).
- [17] R. Rahman, G. P. Lansbergen, J. Verduijn, G. C. Tettamanzi, S. H. Park, N. Collaert, S. Biesemans, G. Klimeck, L. C. L. Hollenberg, and S. Rogge, Electric field reduced charging energies and two-electron bound excited states of single donors in silicon, *Phys. Rev. B* **84**, 115428 (2011).
- [18] M. J. Calderón, J. Verduijn, G. P. Lansbergen, G. C. Tettamanzi, S. Rogge, and B. Koiller, Heterointerface effects on the charging energy of the shallow  $D^-$  ground state in silicon: Role of dielectric mismatch, *Phys. Rev. B* **82**, 075317 (2010).
- [19] W. Kohn and J. Luttinger, Theory of donor states in silicon, *Phys. Rev.* **98**, 915 (1955).
- [20] A. Ramdas and S. Rodriguez, Spectroscopy of the solid-state analogues of the hydrogen atom: Donors and acceptors in semiconductors, *Rep. Prog. Phys.* **44**, 1297 (1981).
- [21] R. Rahman, G. P. Lansbergen, S. H. Park, J. Verduijn, G. Klimeck, S. Rogge, and L. C. L. Hollenberg, Orbital Stark effect and quantum confinement transition of donors in silicon, *Phys. Rev. B* **80**, 165314 (2009).
- [22] A. Szabo and N. S. Ostlund, *Modern Quantum Chemistry: Introduction to Advanced Electronic Structure Theory* (Dover Publications, Inc. Mineola, New York, 2012).
- [23] J. Slater and G. Koster, Wave functions for impurity levels, *Phys. Rev.* **94**, 1498 (1954).
- [24] R. Rahman, C. J. Wellard, F. R. Bradbury, M. Prada, J. H. Cole, G. Klimeck, and L. C. L. Hollenberg, High Precision Quantum Control of Single Donor Spins in Silicon, *Phys. Rev. Lett.* **99**, 036403 (2007).
- [25] S. Ahmed, N. Kharche, R. Rahman, M. Usman, S. Lee, H. Ryu, H. Bae, S. Clark, B. Haley, M. Naumov *et al.*, in *Encyclopedia of Complexity and Systems Science* (Springer, New York, 2009), pp. 5745–5783.
- [26] S. Lee, L. Jönsson, J. W. Wilkins, G. W. Bryant, and G. Klimeck, Electron-hole correlations in semiconductor quantum dots with tight-binding wave functions, *Phys. Rev. B* **63**, 195318 (2001).
- [27] R. Yokota and L. A. Barba, *Treecode and Fast Multipole Method for N-Body Simulation with CUDA*, GPU Computing Gems Emerald Edition (Morgan Kaufmann, Burlington, MA, 2011), Chap. 9, p. 113.
- [28] E. Nielsen, R. Rahman, and R. P. Muller, A many-electron tight binding method for the analysis of quantum dot systems, *J. Appl. Phys.* **112**, 114304 (2012).
- [29] J. Salfi, J. Mol, R. Rahman, G. Klimeck, M. Simmons, L. Hollenberg, and S. Rogge, Spatially resolving valley quantum interference of a donor in silicon, *Nat. Mater.* **13**, 605 (2014).
- [30] G. Lansbergen, R. Rahman, C. Wellard, I. Woo, J. Caro, N. Collaert, S. Biesemans, G. Klimeck, L. Hollenberg, and S. Rogge, Gate-induced quantum-confinement transition of a single dopant atom in a silicon FinFET, *Nat. Phys.* **4**, 656 (2008).
- [31] M. Taniguchi and S. Narita,  $D^-$  state in silicon, *Solid State Commun.* **20**, 131 (1976).
- [32] T. B. Boykin, G. Klimeck, and F. Oyafuso, Valence band effective-mass expressions in the  $sp^3d^5s^*$  empirical tight-binding model applied to a Si and Ge parametrization, *Phys. Rev. B* **69**, 115201 (2004).
- [33] M. J. Calderon, B. Koiller, X. Hu, and S. DasSarma, Quantum Control of Donor Electrons at the Si – SiO<sub>2</sub> Interface, *Phys. Rev. Lett.* **96**, 096802 (2006).

- [34] M. J. Calderón, A. Saraiva, B. Koiller, and S. Das Sarma, Quantum control and manipulation of donor electrons in Si-based quantum computing, *J. Appl. Phys.* **105**, 122410 (2009).
- [35] G. Pica, B. W. Lovett, R. N. Bhatt, T. Schenkel, and S. A. Lyon, Surface code architecture for donors and dots in silicon with imprecise and nonuniform qubit couplings, *Phys. Rev. B* **93**, 035306 (2016).
- [36] B. Voisin, J. Salfi, J. Bocquel, R. Rahman, and S. Rogge, Spatially resolved resonant tunneling on single atoms in silicon, *J. Phys.: Condens. Matter* **27**, 154203 (2015).
- [37] J. Salfi, B. Voisin, A. Tankasala, J. Bocquel, M. Usman, M. Simmons, L. Hollenberg, R. Rahman, and S. Rogge, Valley filtering and spatial maps of coupling between silicon donors and quantum dots, [arXiv:1706.09261](https://arxiv.org/abs/1706.09261).
- [38] B. Voisin, M. Cobian, X. Jehl, M. Vinet, Y.-M. Niquet, C. Delerue, S. deFranceschi, and M. Sanquer, Control of the ionization state of three single donor atoms in silicon, *Phys. Rev. B* **89**, 161404 (2014).
- [39] J. Towns, T. Cockerill, M. Dahan, I. Foster, K. Gaither, A. Grimshaw, V. Hazlewood, S. Lathrop, D. Lifka, G. D. Peterson, R. Roskies, J. R. Scott, and N. Wilkins-Diehr, XSEDE: Accelerating Scientific Discovery, *Comput. Sci. Engg.* **16**, 62 (2014).